



Contents lists available at ScienceDirect

Reliability Engineering and System Safety

journal homepage: www.elsevier.com/locate/ress

An asset management modelling framework for wind turbine blades considering monitoring system reliability

Wen Wu^{a,*}, Darren Prescott^b, Rasa Remenyte-PreScott^b, Ali Saleh^c, Manuel Chiachio Ruano^c^a Institute for Aerospace Technology & Resilience Engineering Research Group, The University of Nottingham, NG7 2RD, United Kingdom^b Resilience Engineering Research Group, Faculty of Engineering, University of Nottingham, University Park, Nottingham, NG7 2RD, United Kingdom^c Department of Structural Mechanics and Hydraulic Engineering, Andalusian Research Institute in Data Science and Computational Intelligence (DaSCI), University of Granada (UGR), Granada 18001, Spain

ARTICLE INFO

Keywords:

Asset management
Wind turbine blades
Petri nets
Structural health monitoring
Monitoring system reliability

ABSTRACT

By incorporating information about asset condition from a monitoring system, engineers can utilize asset management models to manage maintenance activities on wind turbine blades throughout their lifespan. This can lower operating and maintenance costs and increase the life of the blades. The asset management model relies on the monitoring system as a source of information, however, commonly the reliability of the monitoring system is not considered. This paper presents a wind turbine blade asset management Petri net (PN) model that covers the blade asset management process, including degradation, inspection, condition monitoring (CM), and maintenance processes. The paper proposes two contributions. Firstly, while taking into account detailed industry guidelines, the developed model can forecast the future blade condition for a given asset management strategy. Secondly, it investigates the impact of the reliability of the monitoring system on the asset management modelling results. With the aid of the developed model, the number of repair actions and probability distributions of blade condition discovery time are obtained. In addition, the PN gives an indication of how misreporting (underestimation and overestimation) occurs and the extent of the misreporting. The simulation results illustrate the degree of uncertainty introduced into the monitoring results by the reliability of the monitoring system and, consequently, the extent to which this factor influences the maintenance strategies. The proposed model can be used to support asset management decisions when monitoring system performance degrades.

1. Introduction

The wind power industry has experienced significant global growth. Wind energy is one of the fastest growing renewable energy sources, with many countries increasingly adopting wind energy as a key component of their energy mix. In June 2023, the world's installed wind energy capacity reached 1 terawatt (TW) [1]. The rapid growth in the wind power sector has presented formidable challenges in the realm of its operational and maintenance practices. The lifespan of a good quality and modern wind turbine is around 20 years [2], hence each decision made during the operating phase can have a significant impact on the project's maintainability [3,4]. Appropriate asset management, relating to wind turbine performance and repairs over their lifetime, can be used to extend the expected lifespan, minimize risk and maximize the value of the investment.

Different inspection tools and structural health monitoring (SHM) systems are used to obtain wind turbine health condition, which can be used to optimize maintenance strategies. Visual, drone and internal

rover inspections are performed regularly every one to two years, with the inspection interval varying with the age of the wind turbines. In contrast to periodic inspections, SHM systems can provide a continuous indication of component condition [5]. In the context of SHM, online detection and characterization leads to a condition-based maintenance approach, where the reliability of the structure can be quantified, and maintenance procedures only performed when necessary [6,7]. Describing how inspections and monitoring systems can be integrated into a decision making process is critical to avoiding unnecessary repair actions.

Due to their flexibility and their capability when simulating dynamic processes, PNs have been applied to model the asset management of wind turbine structures [8,9]. For example, a PN-based offshore wind turbine maintenance model was developed in [10]; they considered three different maintenance strategies in detail: corrective maintenance, periodic maintenance, and condition-based maintenance. Müller [11] presented a close-to-reality maintenance optimization

* Corresponding author.

E-mail address: wen.wu1@nottingham.ac.uk (W. Wu).

<https://doi.org/10.1016/j.ress.2024.110478>

Available online 31 August 2024

0951-8320/© 2024 The Authors. Published by Elsevier Ltd. This is an open access article under the CC BY-NC license (<http://creativecommons.org/licenses/by-nc/4.0/>).

model using high-level PNs; different detailed points were considered, e.g. the joint use of maintenance capacities, as well as aspects relating to spare parts logistics or weather. Santos [12] presented an age-dependent preventive maintenance model with an imperfect repair strategy. Le [13] proposed an asset management model based on the PN method for modelling offshore wind turbine reliability accounting for degradation, inspection and maintenance processes. Saleh [14] proposed an intelligent Petri net method integrating PNs with reinforcement learning, which can maximize reliability and availability by finding an optimal O&M policy. A PN simulation model was developed to evaluate the availability of offshore wind turbines, as well as their O&M costs in [15]. This study involved a detailed exploration of the influence of a purpose-designed CM system and a Supervisory Control and Data Acquisition (SCADA)-based CM system, both individually and in various combinations, alongside an analysis of diverse maintenance strategies. Various high-level PNs were also developed to extend their simulation capabilities in other application areas [16,17]. The stochastic PNs were used in [18] to model and evaluate of gas leakage emergency rescue process in gas transmission station. Saleh [19] has introduced an Intelligent PN model by merging PN with Reinforcement Learning to consider the maintenance and operation of railway sections. The model is able to use diverse information, including usage, degradation rates, maintenance effectiveness, fault probabilities, and maintenance time, to simulate and learn at the same time. Hadri and Prescott [20] developed a novel modularized Coloured Hybrid PN modelling framework that can be applied to assess system performance under various asset management strategies including condition-based maintenance and risk-based maintenance. In [21], PN model is applied to tackle all aspects of nuclear safety, spanning from design, operation, and maintenance to accident response and recovery, in the case of high-impact low-probability events. In summary, here are three reasons why we use the PN method in our work. Firstly, PNs are ideally suited to modelling dynamic systems with discontinuous state changes [22], such as blade repair processes under different defect severities. Secondly, PNs help visualize and provide a graphic description of a system [22]. From the constructed PNs, we can clearly see the overall situation of wind turbine asset management, such as the number of defects, the progression of defect degradation, and the repair process. Finally, PNs are flexible and can be readily expanded. For instance, the failure model can incorporate various types of failure history data, such as time-series failure data and failure rates. This model can be effortlessly extended to simulate the degradation process in various defects and failure modes effectively.

An important part of modelling is describing how SHM functions as part of an asset management process. Furthermore, systems may produce accurate or inaccurate health status information. When do they produce correct or incorrect information? What constitutes an incorrect status? What are the consequences if the CM system provides incorrect output? In order to answer these, and other questions, it is crucial to investigate how asset management outcomes are affected by the monitoring system accuracy. Recent works have also considered the monitoring system degradation in the scope of reliability analysis. Nielsen [23] presented a case study on risk-based maintenance of wind turbine blades, which studied how the potential benefits of SHM systems affect maintenance. Mukhopadhyay [24] highlighted the importance of sensor degradation in system reliability evaluation, and also evaluated the remaining life of degrading systems monitored by degrading sensors. Some researchers have included information modelling into reliability analysis. Nielsen [25] offered an operational framework for dealing with problems where the extent of true and false information cannot be ascertained a priori. In [26,27] the value of information associated with information collection has been modelled and the effect of introducing biases and dependencies on the value of information has been evaluated. Though efforts have been devoted to SHM system reliability, there is still significant room for further exploration due

to the lack of modelling techniques for predicting incorrect/correct monitoring outcomes and their effects.

With the aim of addressing these problems, in this study, a wind turbine blade asset management PN model incorporating risk-based maintenance and structural health monitoring processes is presented. A stochastic process fitted with failure parameters serves as a versatile framework for characterizing the failure progression of various defects, offering adaptability to different defect types. The PN module within monitoring systems, encompassing inspection and CM, is designed to be practical in its application. Specifically, the incorporation of stochastic, unknown defect into the inspection module is a notable feature. Within the CM module, consideration is given to the dynamic evolution of monitoring accuracy over time and diverse monitoring discovery paths, thereby encompassing the influence of monitoring system reliability. The design of the repair module meticulously adheres to industry standards for defect classification and repair strategies. The utilization of these modules in simulation enables a comprehensive visualization of the asset management process. Additionally, the model accommodates various failure scenarios within the monitoring system to effectively illustrate their impact on system reliability. Ultimately, the model's detailed output regarding state discovery and maintenance strategies serves as a valuable reference for predictive maintenance and managerial decision-making.

In summary, the paper introduces three innovative aspects:

- Firstly, it presents a wind turbine blade asset management PN model incorporating risk-based maintenance and structural health monitoring processes. The PN modules are designed to incorporate industrial guidelines, enhancing their alignment with practical scenarios.
- Secondly, a CM module that considers the reliability of the monitoring system is developed using probability transitions. This module involves the dynamic evolution of monitoring accuracy over time and various monitoring discovery paths.
- Finally, the model thoroughly investigates how asset management outcomes are influenced by the accuracy of the monitoring system, detailing the effects of both correct and incorrect information produced by the system, and how inaccurate outputs are generated by the CM system.

The manuscript is organized as follows. Section 2 gives a general description of the research scope and introduces the basic concepts of the PN method. A PN modelling framework for wind turbine blade asset management is presented in Section 3. In Section 4 and Section 5, results and discussion are provided. Conclusions are presented in Section 6.

2. Background

2.1. Problem description

Wind turbines are complex machines designed to capture kinetic energy from the wind and convert it into electrical energy. They consist of various components that work together to achieve this goal. The rotor blade is a key component of a typical wind turbine, and costs about 20% of the value of the whole machine. The many distinct components that make up a wind turbine each have their own monitoring and management procedures. Here, we focus on wind turbine blades. They have a lengthy lifespan, so engineers can benefit from inspection and CM tools to keep track of the blades' current state. CM and discontinuous periodic inspection are the two main types of monitoring technology that are analysed, often. Ping Monitor, Acoustic Emission, and Ultrasonic Guided Wave Monitoring are examples of CM [28–30]. Internal and annual drone inspections are examples of discontinuous inspection methods [31,32]. The areas that different technologies are responsible for monitoring are also distinct, as are their roles. Failures of the CM system are taken into consideration here.

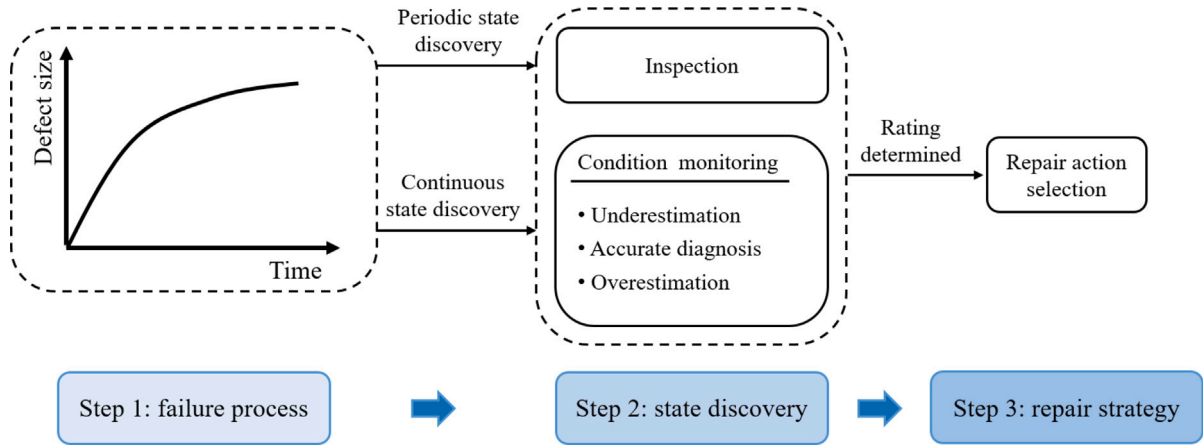


Fig. 1. Overview of the workflow examined in this paper.

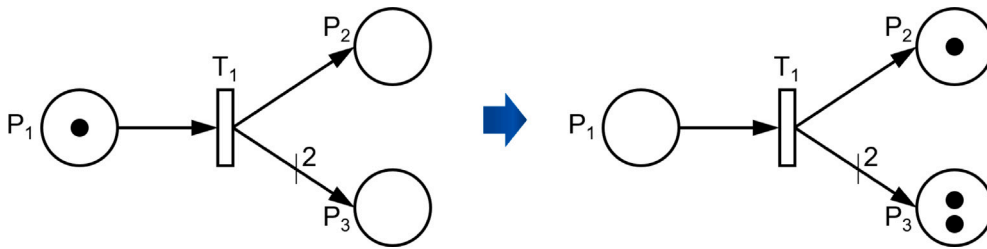


Fig. 2. A simple PN model before and after transition firing.

Based on the above description, the overview of the workflow examined in this paper is shown in Fig. 1. The asset management model consists of three integral steps: the degradation modelling process, the discovery of states through inspection and CM tools, and the selection of repair strategies predicated on defect ratings.

2.2. Petri net concepts

PNs are directed, bipartite, graphical and mathematical modelling tools, consisting of four simple elements: places, transitions, arcs, and tokens. The PN is described by circular nodes, called places, and rectangular nodes, called transitions, with a number of directed arcs connecting places and transitions. The state of a PN is described by its marking, which is defined according to the distribution of tokens in the places. Tokens are moved from, or added to places based on firing rules. A transition is enabled if all of its input places are marked with a required number of tokens defined by the weight of the corresponding connecting arcs. The transition can fire immediately or after a specified delay. Firing removes an arc weight amount of tokens from each input place and adds an arc weight amount to each output place [33,34].

To aid understanding, a simple example is given in Fig. 2. The left side is the initial state. In this paper, Place 1 will be referred to as P₁, transition 1 as T₁ and so on. In this PN, T₁ has one input place, P₁, and two output places, P₂ and P₃. Since P₁ is initially marked, the transition is enabled and after a delay, it will fire. During firing, one token is removed from P₁ and one/two tokens added to P₂ and P₃ respectively, due to the weight of the arcs connecting each of them to T₁. The state after firing is shown on the right side.

To simulate the CM tool error, a probabilistic transition is introduced, which models different monitoring outcomes based on their probabilities. Probability transitions add tokens to their output places with a certain probability, which is associated with the corresponding arcs, with the probability of all of the output arcs of a single probability transition adding to 1. Probabilistic transitions are described in

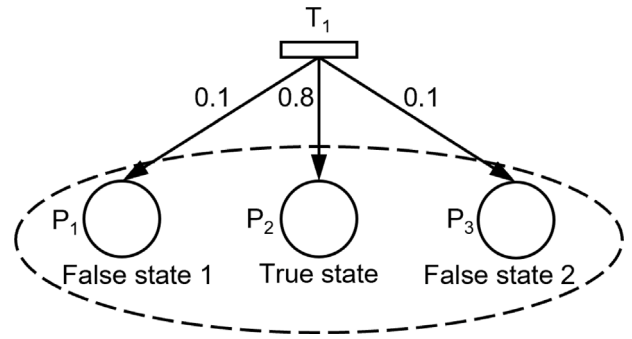


Fig. 3. A PN model containing a probabilistic transition.

detail in [35]. When a probability transition fires, a token is randomly added to one of its output places based on the assigned probabilities. The probability of token movement is determined by the monitoring accuracy of the monitoring system. For instance, with a monitoring accuracy of 0.8, the probability of the control token moving to a place indicating a true discovery is set to 0.8. Furthermore, it is assumed that the probability of moving to both false states (either underestimation or overestimation the severity of the reported degradation) is equal. Hence, the probabilities of moving to the two false states would be set to 0.1. All the output places of a probability transition will be surrounded by a dashed ellipse.

A probabilistic transition example is shown in Fig. 3. When T₁ fires, the probabilities of the token moving to P₁, P₂ and P₃ are 0.1, 0.8 and 0.1, respectively. A monitoring system represented by T₁ has an 80% probability of discovering the true state of the monitored blade, and a 10% probability of reporting false state 1 and false state 3, respectively. If a token is added to P₁, the state identified by the monitoring system is state 1, and so on.

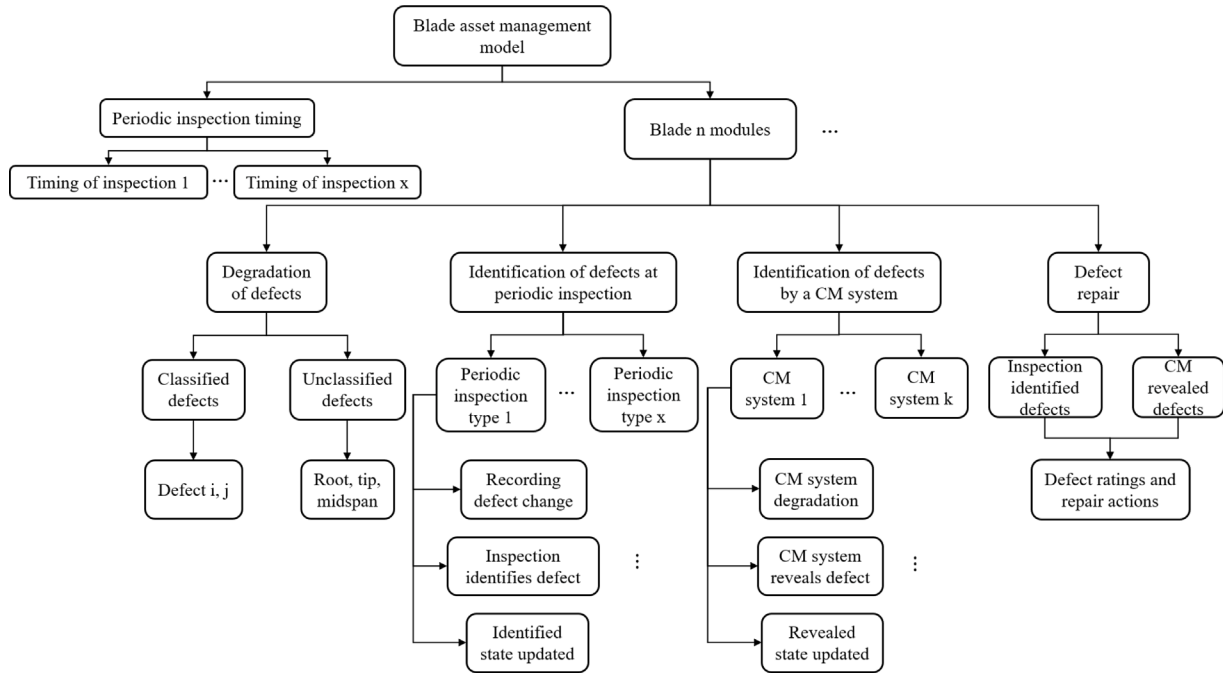


Fig. 4. Proposed asset management model structure.

3. PN model of wind turbine blade asset management

In this section, the asset management model for wind turbine blades is presented. It consists of four modules: a degradation module, an inspection module, a CM module and a maintenance module. A tree diagram of the proposed asset management model structure is shown in Fig. 4.

According to the survey in [36], there are more than 17 different types of defect that could occur to each blade. Possible defects discovered during periodic inspections include leading edge erosion, lightning delamination, trailing edge transverse laminate cracks and other defects in the outer surface of the blade. Possible defects revealed by CM include shear web cracking and delamination, bondline failure along the spar box or shear web to spar, and other damage occurring inside the blade. These named defects are called classified defects. Unclassified defects are defined as defects that are unnamed or have not been previously discovered. In this section, defects identified during inspections and revealed by the CM system are denoted as i and j , respectively. The condition of the wind turbine blade will be assigned by engineers based on the severity of the observed defect. The industry handbook that was adapted to develop the rating system shown in Table 1 was published to provide a common understanding of words, process, levels and concepts to all parties involved in the research and development of wind turbine blades [37]. Repair strategies are determined based on these overall ratings rather than the actual size of the defect.

3.1. Degradation modules

In this section, the degradation modules of classified and unclassified defects identified using inspection and revealed using CM are presented.

3.1.1. Degradation relating to classified defects

This module models the degradation of wind turbine blades according to defect growth and an instance of this module will be included in the PN model for each classified defect i that is modelled.

Places represent different defect size ranges, and transitions govern the transition times between different states (see Fig. 5). The places from $P_{i,1}$ to $P_{i,5}$ represent the physical growth of defect i from severity 1 to severity 5. Transitions $T_{i,1}$ to $T_{i,4}$ model the progression of the defect from one severity to next. Place $P_{i,x}$ is marked when a change in defect severity occurs and is connected to the inspection module to increase the efficiency of the Monte Carlo simulation analysis of the PN, detailed explanation will be provided in Section 3.2. A similar place appears in the degradation module for each defect type that is discovered at the same inspection as defect i .

3.1.2. Occurrence of unclassified defects

In real-world scenarios, unclassified defects may occur, which are subsequently detected at inspection, for example, during the examination of photos taken by drones. These defects are unusual and tend to lack established degradation parameters for characterizing the failure progression. Consequently, defect ratings are assigned based on the specific location of these defects. The module designed for simulating the occurrence of an unclassified defect is presented in Fig. 6. Transition $T_{i,35}$ is a probabilistic transition, and will fire after a time interval defined according to industrial experience. Places, $P_{i,29}$, $P_{i,30}$, and $P_{i,31}$ symbolize unclassified defects that have emerged at different locations, specifically at the root, midspan, and tip of the blade. $P_{i,x}$ is marked to indicate within the module that there is an unclassified defect to be discovered at periodic inspection type x .

3.1.3. Degradation relating to defects identified using the CM system

A similar module to that used to model classified defects is adapted to model the growth of defects whose presence is monitored using the CM system, as shown in Fig. 7. However, in this case, a place corresponding to $P_{i,x}$ is not required, since the operation of the CM system must be modelled at regular, short intervals.

3.2. Periodic inspection modules

Inspection aims to identify different types of defects, alongside randomly occurring, unclassified defects. Fig. 8 to Fig. 13 provide a

Table 1
Defect ratings and corresponding repair actions.
Source: Adapted from [37].

Ratings	Defect description	Repair action
Rating 1	No defect or cosmetic damage	No need for immediate action
Rating 2	Outside of tolerance, but low potential for growth	Repair if nearby defects are to be repaired (Type I)
Rating 3	Outside of tolerance where there is potential for growth	Repair in 10–16 months (Type II)
Rating 4	Serious defect outside of tolerance affecting structural integrity	Monitor regularly until the repair performed in 3 months (Type III)
Rating 5	Critical defect with severe structural integrity loss	Stop turbine and repair/replace (Type IV)

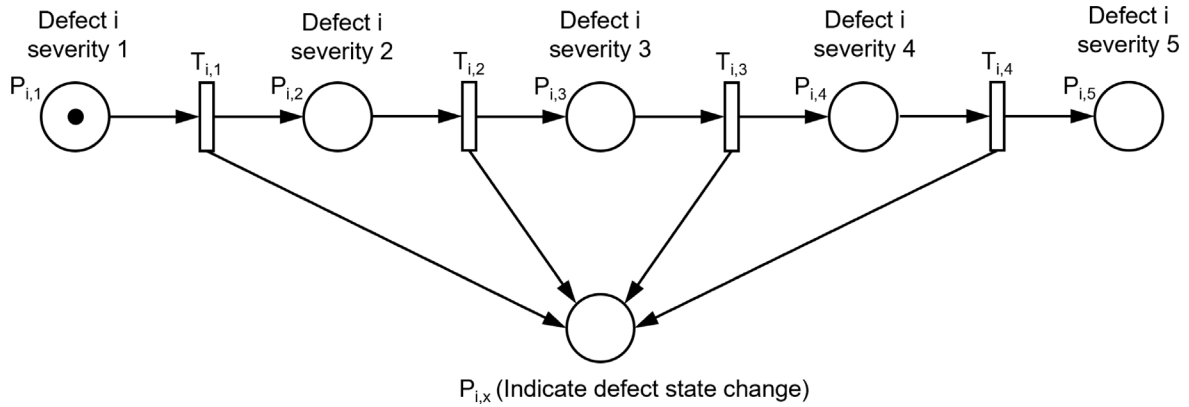


Fig. 5. PN describing the growth of classified defect i.

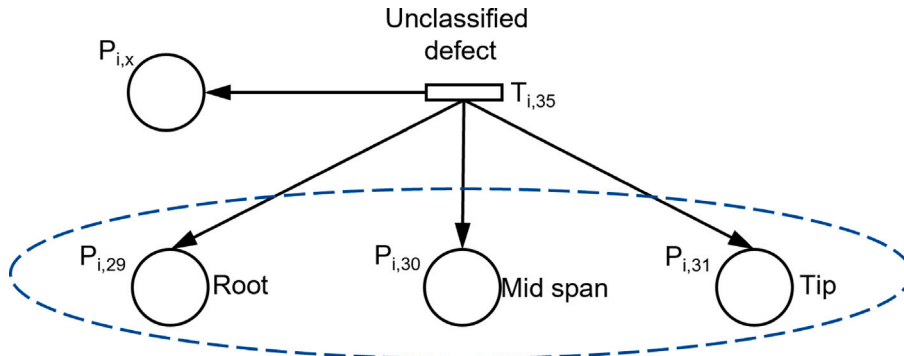


Fig. 6. PN describing the occurrence of an unclassified defect.

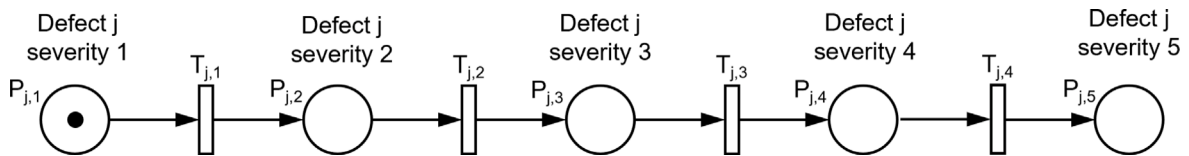


Fig. 7. PN describing the growth in severity of defect j, whose presence is monitored using the CM system.

visual representation of the inspection process within the PN modelling framework.

3.2.1. Recording defect state changes

Although, in practice, inspections take place periodically, within the PN an inspection is only modelled if a change in state will be

discovered, which is the minority of inspections. The place $P_{i,x}$, already depicted in Figs. 5 and 6, registers the occurrence of a change in defect severity that should be discovered at periodic inspection type x. The PN module shown in Fig. 8 marks place $P_{x,\sigma}$, which is used to indicate that at least one of the defects that is tracked at the periodic inspections has experienced at least one change in severity. If $P_{i,\sigma}$ is empty when

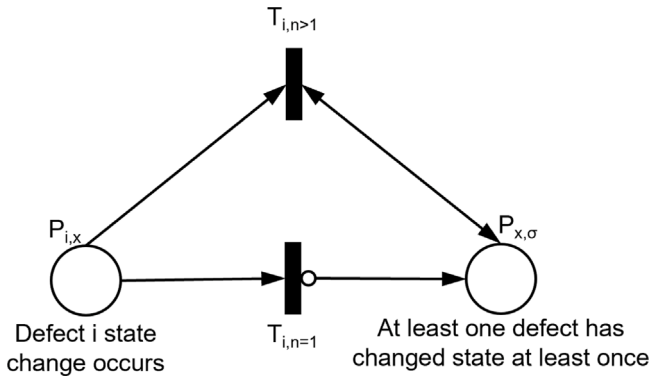


Fig. 8. PN to record defect state changes.

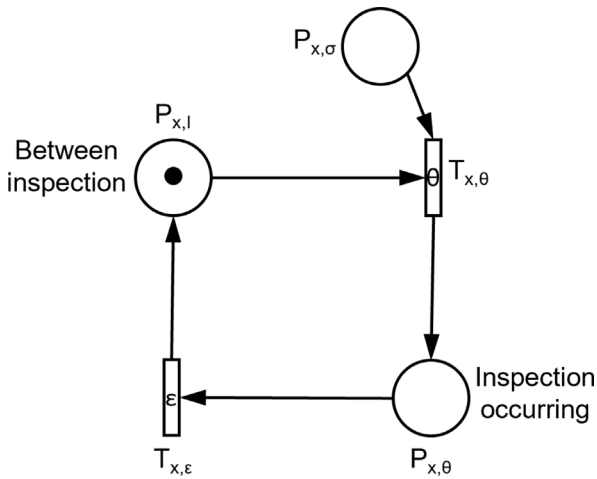


Fig. 9. PN describing the timing of inspection process.

$P_{i,x}$ becomes marked, $T_{i,n=1}$ immediately empties $P_{i,x}$ and marks $P_{x,\sigma}$ to signify that at least one change in defect severity has occurred since the last inspection. If $P_{x,\sigma}$ is already marked, meaning that there has already been at least one change in the severity of at least one defect since the last inspection, then $T_{i,n}$ will unmark $P_{i,x}$. $T_{i,n>1}$ ensures that $P_{x,\sigma}$ contains at most a single token. A similar module exists for all defects whose presence is discovered and tracked at periodic inspections type x , with the place $P_{x,\sigma}$ being common to them all.

3.2.2. Timing of inspections

Fig. 9 shows the inspection process for defect i , which is discovered at period inspection x . The delay time associated with $T_{x,\theta}$ is periodic inspection interval and the delay time associated with $T_{x,\epsilon}$, ϵ , is a modelling delay, which in practice is equivalent to 0, but has an infinitely small delay for the purpose of the modelling in order to ensure that transitions fire in the correct order, with all inspections carried out before $T_{i,\epsilon}$ fires and ends the inspection. The inspection only happens at $\theta, 2\theta$ and so on, meaning that the delay associated with $T_{x,\theta}$ must be set to ensure a firing time that is a multiple of θ . $P_{x,l}$ is thus marked when an inspection is being carried out, and $P_{x,\sigma}$ is marked between inspections. Although inspections take place in practice at regular intervals, within the PN model the inspection only takes place if there is a change in defect state to be discovered, which is achieved by connecting $P_{x,\sigma}$ to $T_{x,\theta}$. This increases the efficiency of the simulation used to analyse the PN, since changes in defect state generally occur less frequently than the inspections and simulation time is not wasted on the modelling of featureless inspections.

3.2.3. Identifying degradation relating to classified defects

3.2.3.1. Inspection reveals change of state of classified defect. Fig. 10 shows how a periodic inspection process reveal the rating of defect i . $T_{i,5}$ to $T_{i,9}$ are immediate transitions that represent the identification of the severity of a defect at inspection and will fire only when an inspection is taking place ($P_{x,\theta}$ is marked) and the defect has not already been identified and rated at this particular level (with one of $P_{i,6}$ to $P_{i,10}$ already marked), with $P_{i,6}$ to $P_{i,10}$ denoting the rating values associated with each of the five severities of defect i , which are observed at inspection.

3.2.3.2. Contribution of classified defects to overall blade rating. The severities of all defects are taken into account when determining the blade ratings. Fig. 11 shows how the five observed severities of defect i , represented by $P_{i,6}$ to $P_{i,10}$, are used to identify a corresponding blade rating from 1 to 5, modelled by $P_{i,16}$ to $P_{i,20}$. The place relating to the observed severity of defect i retains its original marking and $P_{i,11}$ to $P_{i,15}$ ensure that $P_{i,16}$ to $P_{i,20}$ can each hold at most one token relating to each defect i . This means that, for example, when two defects are modelled, these places will contain a total of two tokens, one for each defect, and the cumulative marking of these five places will be used to determine the overall blade rating.

3.2.3.3. Updating revealed state for classified defects. The groups of places relating to the severity of defect i ($P_{i,6}$ to $P_{i,10}$) and the overall blade rating ($P_{i,16}$ to $P_{i,20}$) must each contain only one token relating to the severity of defect i to ensure that when a new level of degradation is detected during an inspection only the more severe level of

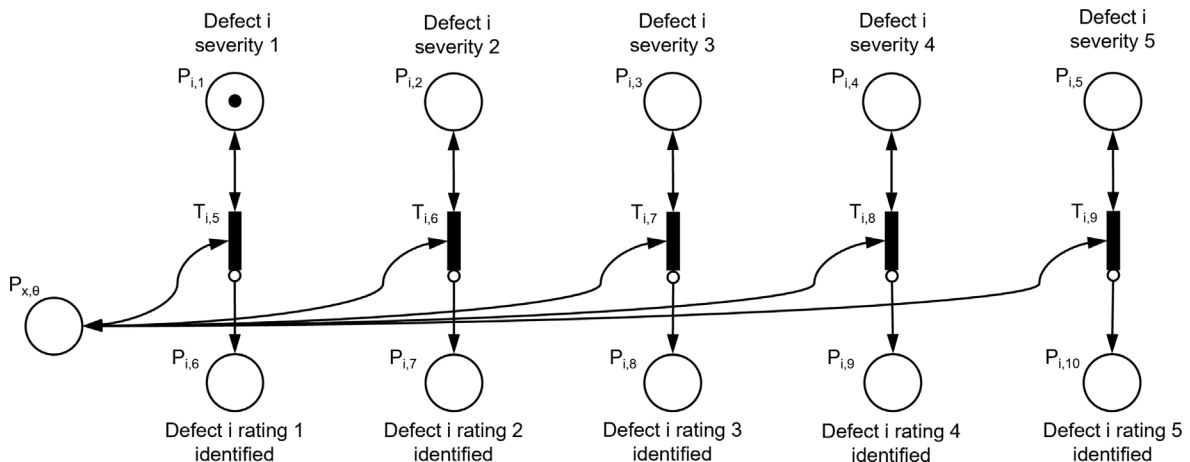


Fig. 10. PN describing the inspection process for defect i .

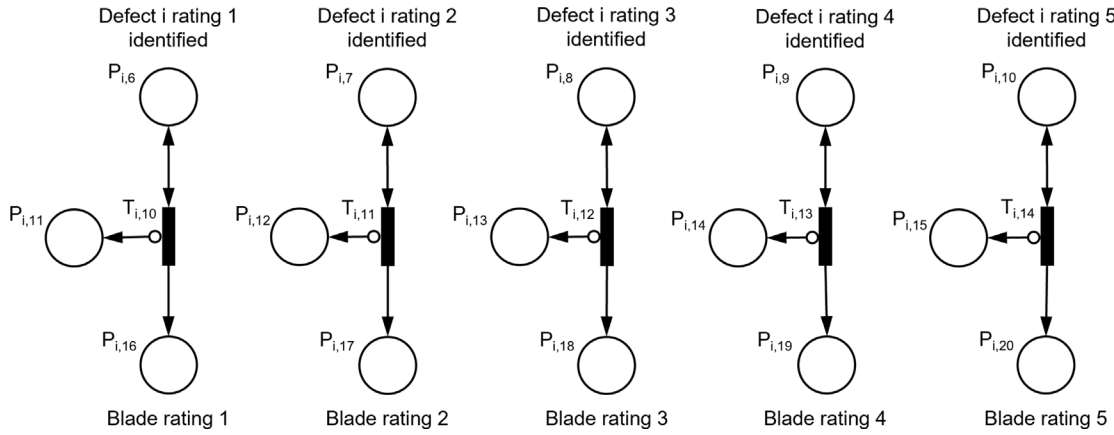


Fig. 11. PN describing the determination of the contribution of defect i to the overall blade rating.

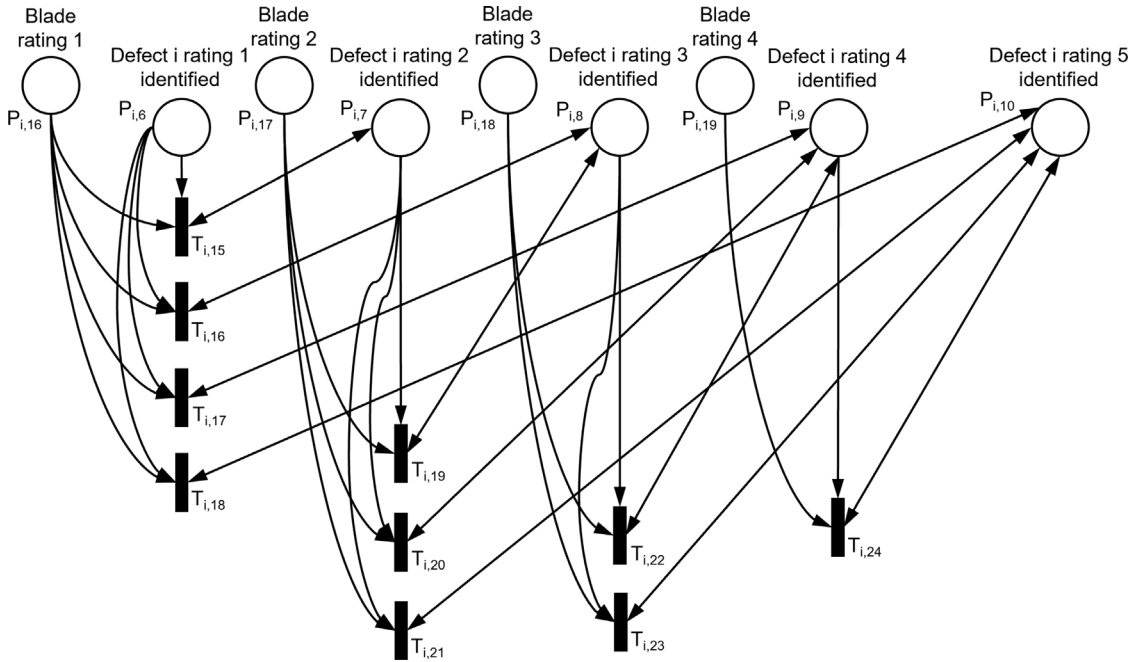


Fig. 12. PN module updating the rating identified for defect i during the inspection process.

degradation is stored within the PN model. This process is handled by the module shown in Fig. 12. Upon the detection of an increased level of degradation during inspection, this module keeps the marking of the place representing the newly identified defect rating while concurrently unmarking places corresponding to previously identified defect ratings. The marking status of each individual defect ($P_{i,6}$ to $P_{i,10}$), and the total ratings ($P_{i,16}$ to $P_{i,20}$) are all updated. For instance, if the current identified state of defect i transitions from rating 2 to rating 3, meaning that $P_{i,8}$ and $P_{i,18}$ are marked by the modules shown in Fig. 10 and Fig. 11, then $P_{i,7}$ and $P_{i,17}$ must be emptied. This is performed by the firing of $T_{i,19}$. The other transitions in this module cover the other possible cases.

3.2.4. Identifying unclassified defects at inspection

Fig. 13 shows the inspection process identifying the existence of unclassified defects. Unlike classified defects, for which degradation is understood and can be modelled, unclassified defects are merely identified to exist or not. Therefore, the module modelling inspection related to unclassified defects can be used to directly identify the contribution of the defect to the overall blade rating. $P_{x,\theta}$ indicates periodic inspection of type x is taking place and $T_{i,36}$ to $T_{i,38}$ model

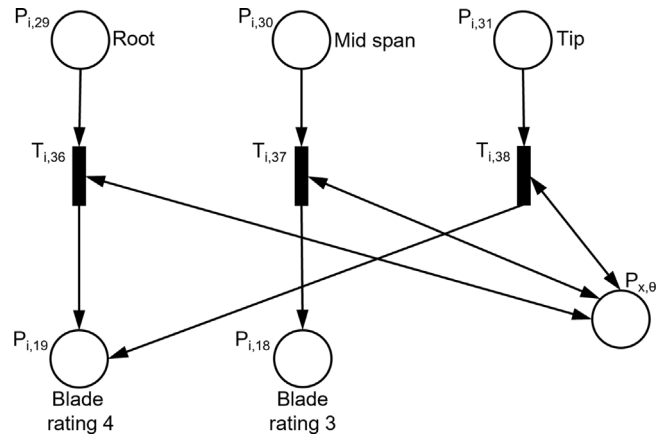


Fig. 13. PN describing the inspection process considering unclassified defects.

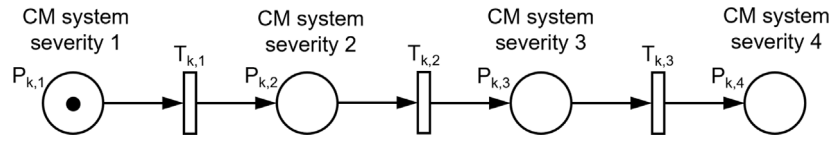


Fig. 14. PN describing the CM system degradation process.

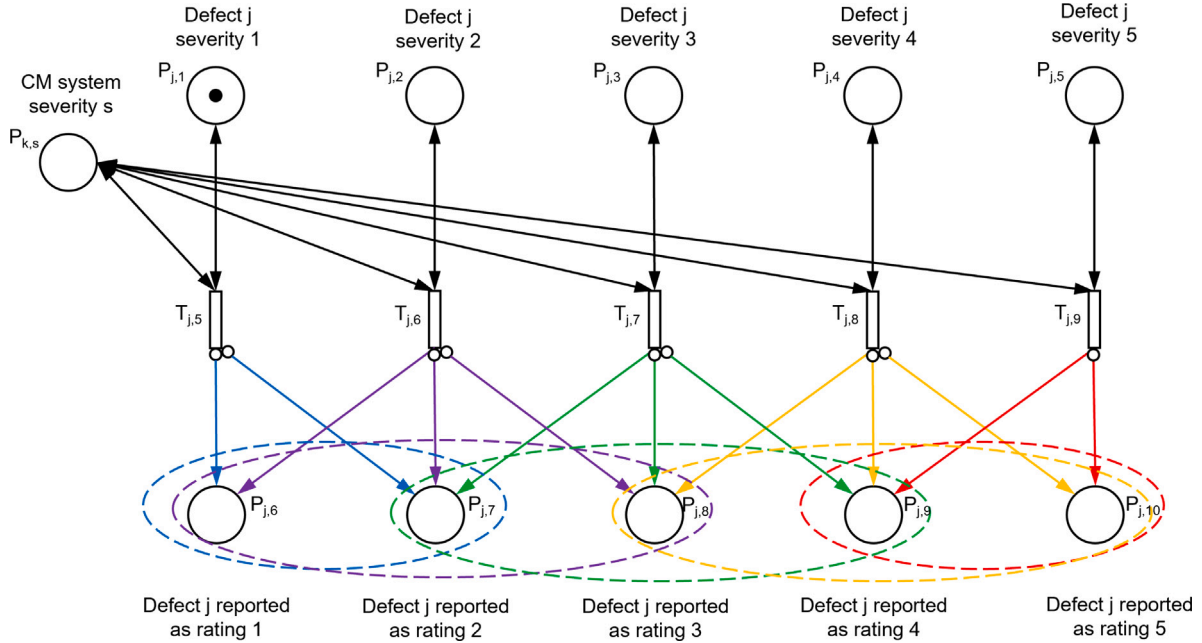


Fig. 15. PN describing the CM process taking into consideration the degradation of the CM system.

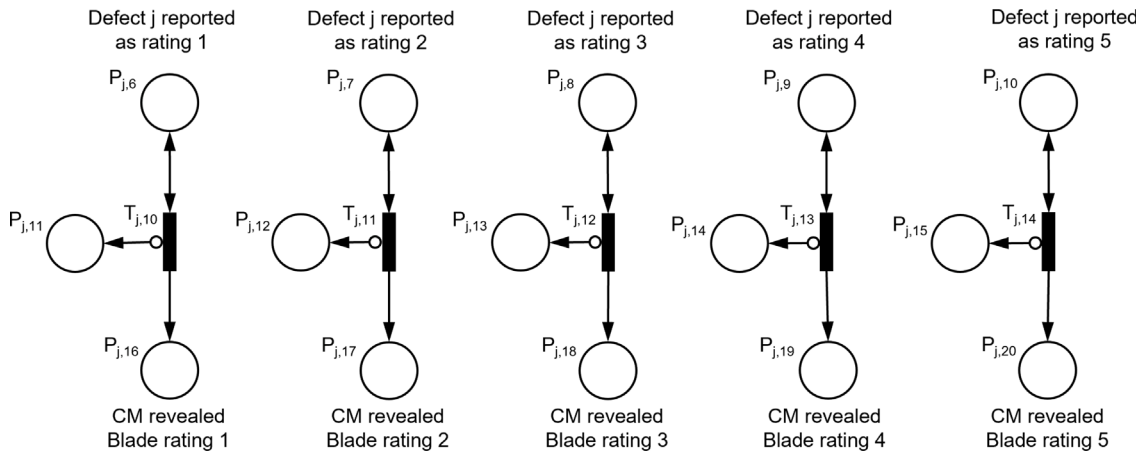


Fig. 16. PN describing the process of a CM system revealing defects.

the discovery of defects at the root, midspan and tip of the blade respectively, which can be immediately identified as contributing to a particular rating. Typically, defects occurring at the root and tip tend to be more severe, and as such, they contribute to a rating of 4, while defects at the midspan result in a rating of 3.

3.3. Condition monitoring (CM) modules

Some defects can only be identified through the continuous monitoring of the blade condition by a CM system. This section presents the PN module dedicated to describing the CM system, as shown from Fig. 14 to Fig. 17. Notably, the module incorporates the consideration of the reliability of the monitoring system.

3.3.1. Degradation of the CM system

The degradation process of the CM system is shown in Fig. 14. The monitoring accuracy of the CM system gradually deteriorates over time due to an increasing probability of sensor failures [24]. $P_{k,1}$ to $P_{k,4}$ denote the four states of the CM system and $T_{k,1}$ to $T_{k,3}$ model the transition of the CM system between these four states. As the CM system degrades, its accuracy reduces. The states of $P_{k,1}$ to $P_{k,4}$ are used by the modules that are used to reveal the occurrence of defects that are identified by the CM system. This is discussed in Section 3.3.2.

3.3.2. CM reveals defect

Fig. 15 shows the CM process for a defect j whose degradation is described in Section 3.1.3. $T_{j,5}$ to $T_{j,9}$ represent the CM system, which

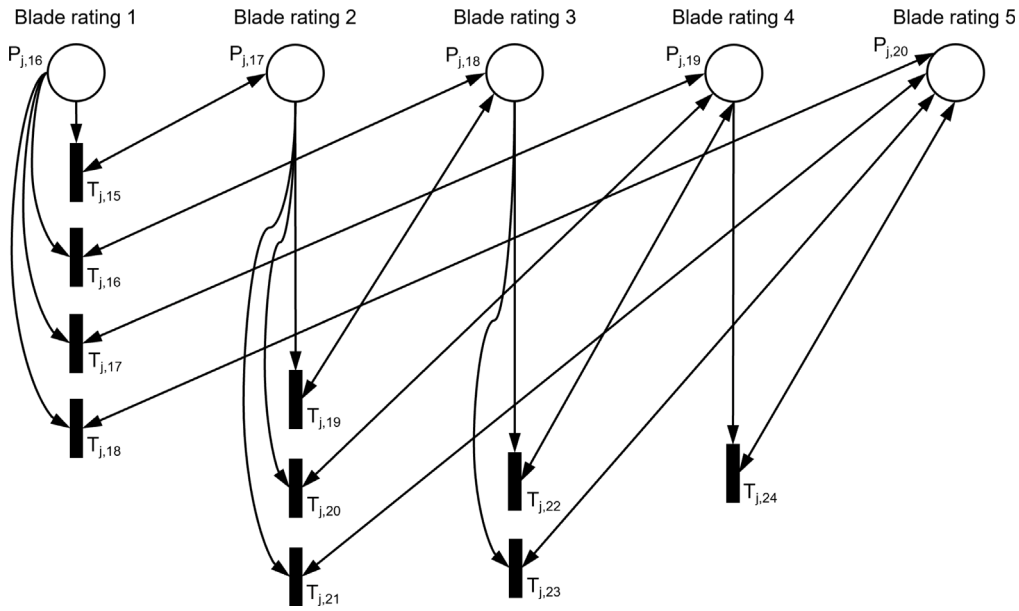


Fig. 17. PN module updating the rating identified by the CM process.

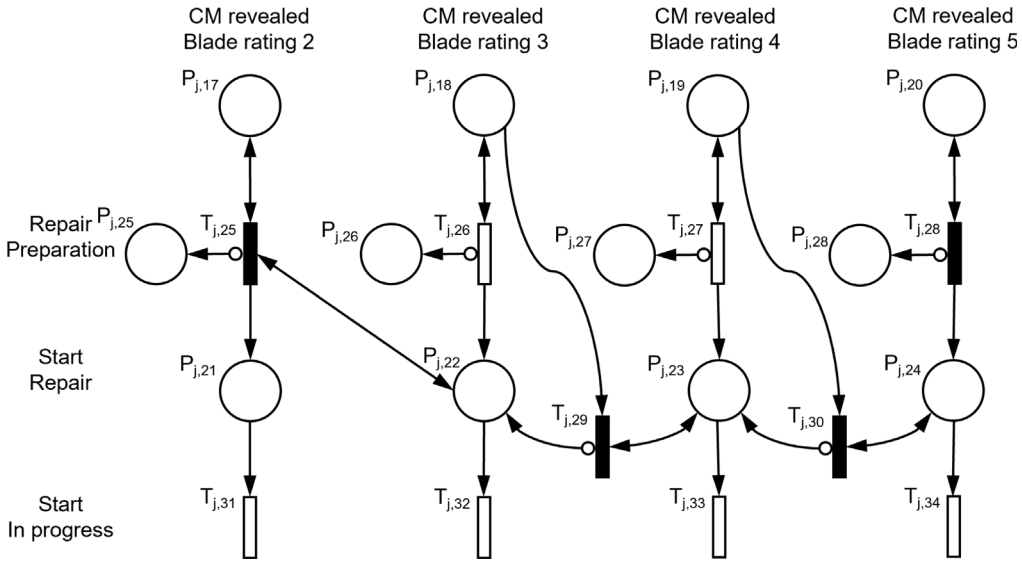


Fig. 18. PN describing repair following the identification of degradation by the CM system.

fires periodically at short intervals, since compared to periodic inspections, CM systems can provide more frequent defect detection. These transitions are linked to five different probabilistic delay transitions, each distinguished by a unique colour. $T_{j,5}$ and $T_{j,9}$ are linked to two potential ratings, while $T_{j,6}$ to $T_{j,8}$ are linked to three, with the output places relating to the possible readings (accurate or inaccurate), that may be reported by the CM system. A similar module exists for each of the CM system severities that are modelled by the PN shown in Fig. 14, with the probabilities of identifying the rating of defect j correctly or incorrectly being specified according to the level of degradation of the CM system. Therefore, for example, when the CM system is degraded to level $P_{k,s}$ (where s is 1 to 4, as shown in Fig. 14), and defect j is of severity 2 (meaning $P_{j,2}$ is marked) then $T_{j,6}$ will be enabled and fire, marking either $P_{j,6}$, $P_{j,7}$ or $P_{j,8}$. Which one of the three is marked depends on the probability of the CM system underestimating the severity (marking $P_{j,6}$), accurately identifying the severity (marking $P_{j,7}$) and overestimating the severity ($P_{j,8}$).

In the event that the CM system provides accurate states, the inhibitor arcs stemming from $P_{j,6}$ to $T_{j,5}$, $P_{j,7}$ to $T_{j,6}$, $P_{j,8}$ to $T_{j,7}$, $P_{j,9}$ to $T_{j,8}$, and $P_{j,10}$ to $T_{j,9}$ function to prevent the repetitive firing of $T_{j,5}$ to $T_{j,9}$. However, if the CM system overstates the detected ratings, the inhibitor arcs extending from $P_{j,7}$ to $T_{j,5}$, $P_{j,8}$ to $T_{j,6}$, $P_{j,9}$ to $T_{j,7}$, and $P_{j,10}$ to $T_{j,8}$ will also inhibit the repetitive firing of $T_{j,6}$ to $T_{j,9}$. This indicates that when the CM system overestimates the defect ratings, a conservative approach is adopted for safety. Consequently, the system will prematurely alert the engineer to perform potentially unnecessary repairs, resulting in additional, unnecessary repair expenses. Conversely, if the CM system underestimates the defect state, the monitoring transitions ($T_{j,5}$ to $T_{j,9}$) will not be inhibited. In this scenario, the CM system will continue to operate until it identifies an accurate or overestimated outcome. Underestimated outcomes mean that the CM may fail to promptly notify engineers to address the defect, which could also lead to unwarranted costs.

The tokens in $P_{j,6}$ to $P_{j,10}$ serve as indicators of the CM system's health status to a certain degree. If the count of tokens in any of

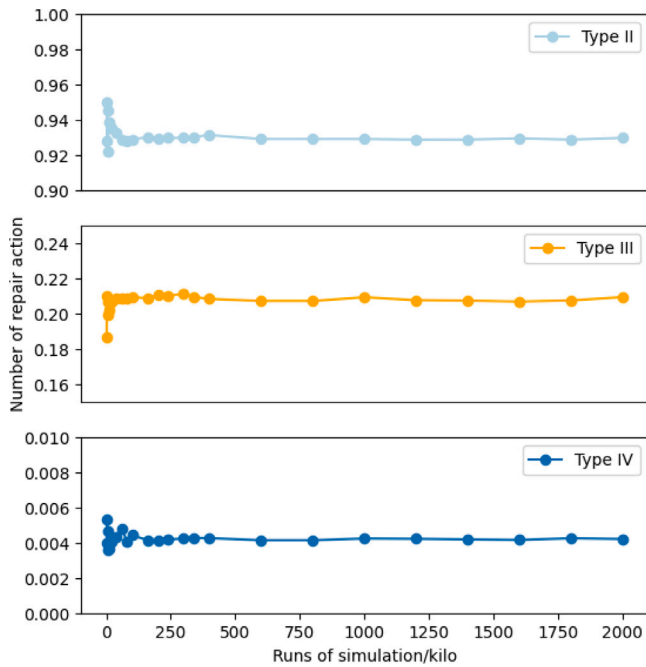


Fig. 19. Average number of different repair actions under different runs of simulation.

these places, ranging from $P_{j,6}$ to $P_{j,10}$, exceeds 1, it signifies an underestimation error by the monitoring system. Conversely, if the token combination is 0 and 1 (for instance, $P_{j,6}$ contains 0 tokens, while $P_{j,7}$ contains 1 token), it indicates an overestimation error made by the monitoring system. In reality, the ratings reported by the CM system would indicate its condition. Based on the PN design here, it would be possible to extend the PN to infer CM system condition as part of a fault diagnosis process in future.

3.3.3. Contribution of defects revealed by CM to overall blade rating

After the CM system has identified the severity of defect j , the blade rating must be updated, as shown in Fig. 16. $P_{j,11}$ to $P_{j,15}$ prevent the repetitive firing of $T_{j,10}$ to $T_{j,14}$. Tokens located in $P_{j,16}$ to $P_{j,20}$ serve to indicate the current blade rating revealed by the CM system, which may diverge from the true state indicated in $P_{j,1}$ to $P_{j,5}$ due to monitoring error.

3.3.4. Updating revealed state for defects identified by CM

Fig. 17 shows a state update module that serves the same purpose as that shown for periodic inspections in Fig. 12. However, a key difference is that the total count of ratings is not updated in this case since only one rating is provided by the CM system.

3.4. Repair module

When defects are detected in terms of their size by the inspection and CM systems, engineers will assign ratings to these defects based on their severity. Subsequently, maintenance decisions will be made in accordance with the criteria outlined in Table 1. As previously mentioned, $P_{i,16}$ to $P_{i,20}$ in the inspection module and $P_{j,16}$ to $P_{j,20}$ in the CM module are linked to the repair module. The repair actions are determined by the number of tokens present in these places. While the places and transitions of the repair modules within the inspection and CM modules are independent, their design is the same. For brevity, only the repair module incorporated within the CM module is depicted, as illustrated in Fig. 18.

Transition $T_{j,25}$, associated with rating 2 defects, cannot be fired independently; it requires notification of other repair actions. Engineers typically address rating 2 defects only when more severe defects also require repair. Additionally, from an economic perspective, it is often more cost-effective to address all defects collectively. Therefore, in the PN design, repairs for lower-rated defects are automatically initiated when repairs for more severe defects commence. For instance, $P_{j,24}$ (indicating the initiation of a rating 5 defect repair) and $P_{j,19}$ (signifying the presence of a rating 4 defect) are linked to $T_{j,30}$. When an engineer initiates the repair of a rating 5 defect, $T_{j,30}$ will fire and add a token to $P_{j,23}$, thereby initiating the repair process for a rating 4 defect. In this paper, rating 2, rating 3, rating 4 and rating 5 defects correspond to different repair strategies and are named Type I, Type II, Type III and Type IV respectively, as shown in Table 1. Transitions $T_{j,26}$ and $T_{j,27}$ represent distinct required waiting periods for repair conditions, which are provided in Table 1. Transition $T_{j,28}$, connected with rating 5 defects, requires immediate repair and is therefore represented by an immediate transition. $P_{j,25}$ to $P_{j,28}$ are utilized to prevent the repetitive firing of $T_{j,25}$ to $T_{j,28}$. The addition of tokens to $P_{j,21}$ to $P_{j,24}$ indicates the initiation of the repair action. Transitions $T_{j,31}$ to $T_{j,34}$ are reset transitions, representing the ongoing maintenance action. If any of these transitions are fired, the defect reverts to its initial condition, signifying that the tokens in the whole module will be reset to their initial state, including $P_{j,1}$ to $P_{j,5}$ (defect severities), $P_{j,6}$ to $P_{j,10}$ (reported defect ratings) and $P_{j,16}$ to $P_{j,20}$ (revealed blade ratings). The reset transitions will do the same for defect i discovered by inspections.

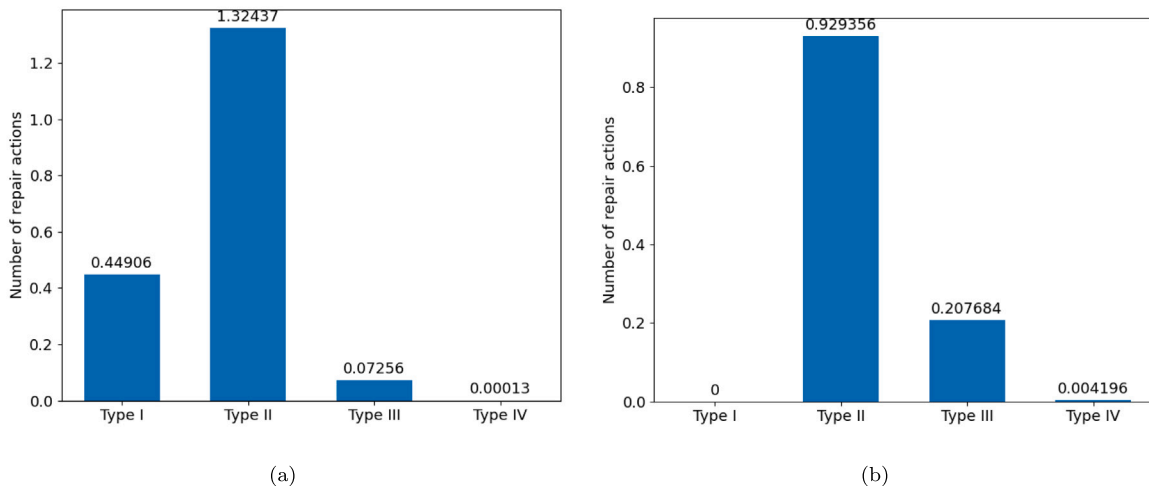


Fig. 20. The average number of repair actions over its lifetime recorded (a) in the inspection module, (b) in the CM module.

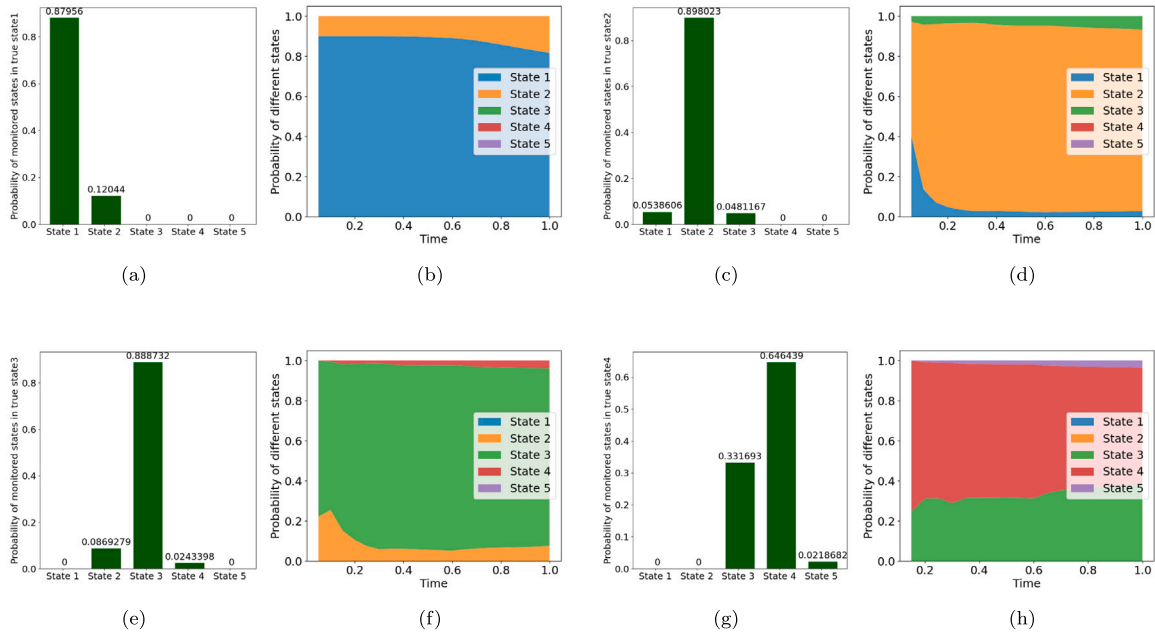


Fig. 21. (a) Probability distribution in true state 1. (b) Probability distribution over time in true state 1. (c) Probability distribution in true state 2. (d) Probability distribution over time in true state 2. (e) Probability distribution in true state 3. (f) Probability distribution over time in true state 3. (g) Probability distribution in true state 4. (h) Probability distribution over time in true state 4.

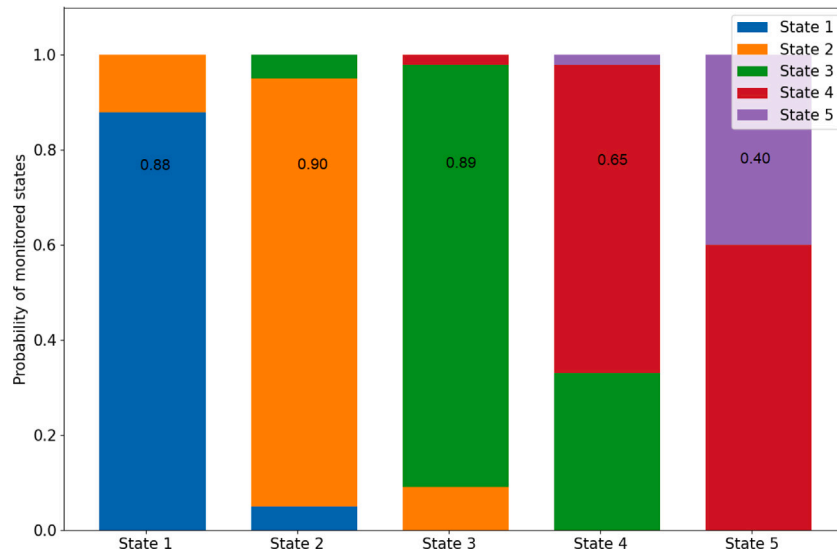


Fig. 22. The overall monitoring accuracy of different states. Marked numbers on the bars represent the monitoring accuracy of each state.

4. Results

4.1. Assumptions and model input parameters

In Section 3, a general asset management model for wind turbine blades is presented, where different modules are introduced, potentially covering various wind turbines, different defect types, different periodic inspection types, and different CM systems. In this section, a case study is provided to illustrate the application of the model. Key assumptions are being made since limited data and sources on wind turbine failures were available [38]:

- The defect evolution data utilized is sourced from historical fatigue load data due to the absence of blade failure data. The delay times for degradation transitions are sampled from Weibull distributions with parameters derived from these data. Transition firing follows a Weibull distribution with scale parameter η and shape parameter β . Approaches for estimating the Weibull parameters can be classified as manual or computational methods [39]. Manual methods perform better for small samples. Additional details on the methodology for acquiring stochastic distribution parameters can be found in [33].
- Three different types of defect are taken into account in this case study. Two of them appear on the outer surface of the blade,

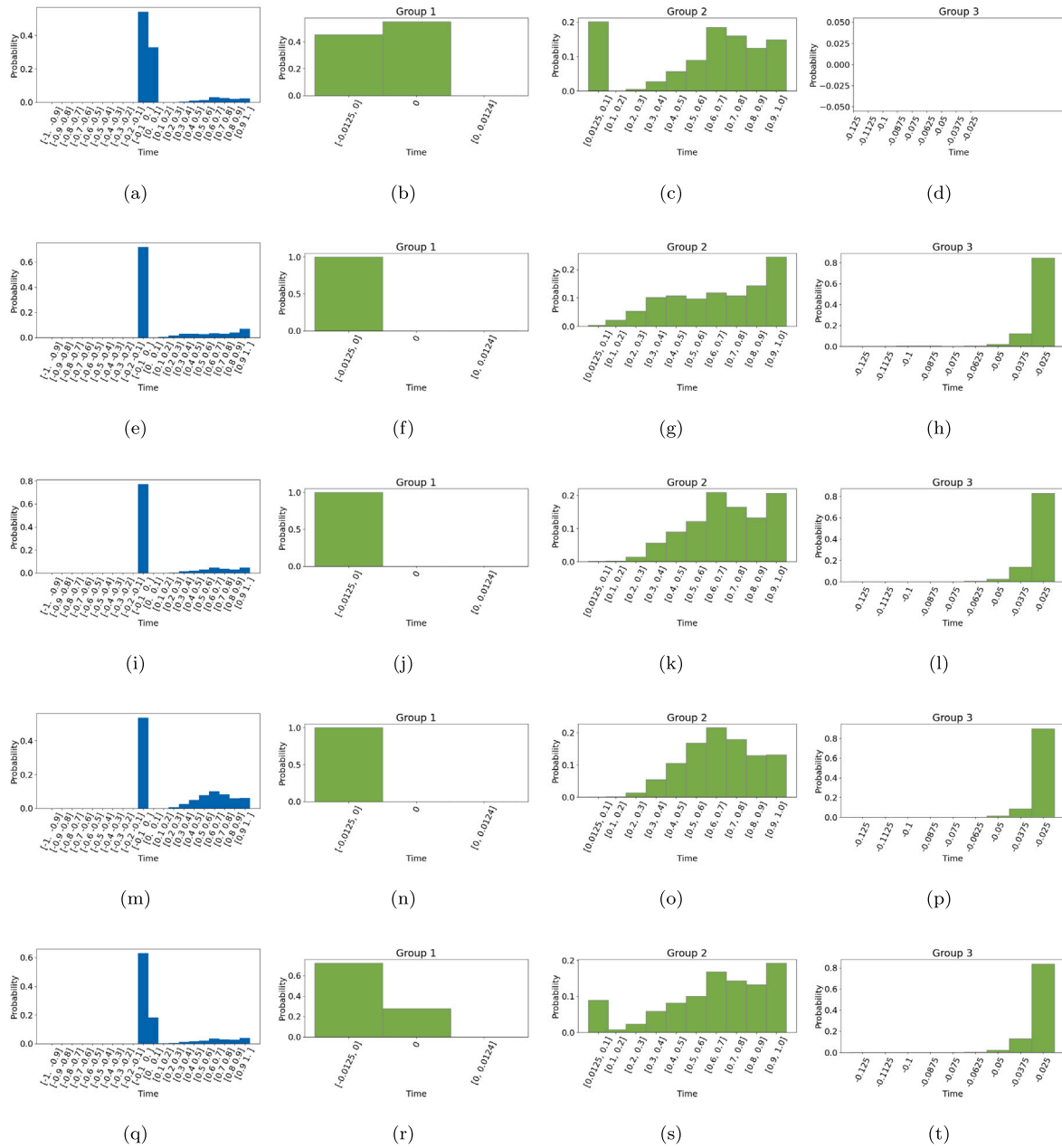


Fig. 23. Probability distribution of state 1 discovery time gap (a) in total, (b) Group 1, (c) Group 2 and (d) Group 3; probability distribution of state 2 discovery time gap (e) in total, (f) Group 1, (g) Group 2 and (h) Group 3; probability distribution of state 3 discovery time gap (i) in total, (j) Group 1, (k) Group 2 and (l) Group 3; probability distribution of state 4 discovery time gap (m) in total, (n) Group 1, (o) Group 2 and (p) Group 3; probability distribution of all states discovery time gap (q) in total, (r) Group 1, (s) Group 2 and (t) Group 3.

which is monitored at a single periodic inspection. The third defect appears inside the blade and is monitored by the CM tool. Also, some unknown defect may occur randomly, which is also taken into account in this paper. The general structure of the model means it can be easily expanded to include further defect types and further inspection.

- The CM system degradation state transitions are governed by constants in the absence of actual data. The initial accuracy of the monitoring system is set to 0.9, and it will gradually decrease to 0.5. This path of monitoring accuracy degradation is considered as path 2. Further details are given in Section 4.6,

which investigates other rates of degradation of the monitoring accuracy.

- It is assumed that the CM system cannot overstate or underestimate the defect severity by more than one rating, and the probabilities of both overestimation and underestimation are considered equal.
- It is assumed that the repair time for defects of different severity levels is governed by constants. The state after the repair is as good as new over time.
- All input parameters in this study have been standardized to unit one in proportion to the 20-year lifespan of wind turbine blades [2].

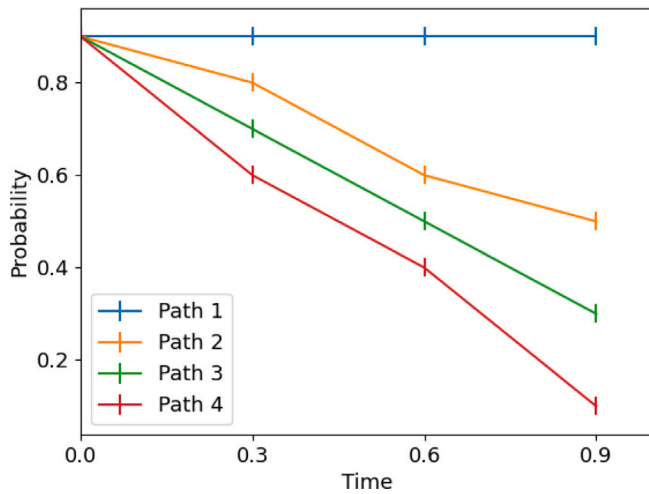


Fig. 24. Different monitoring accuracy paths of the monitoring system.

The input parameters and description of the transitions and places are given in Appendix A.

4.2. Convergence analysis

Monte Carlo simulation is employed to analyse the developed PNs. The convergence criterion is determined by whether the count of distinct repair actions based on the results of the monitoring system reaches a constant or stable value. The evolution of the number of different repair actions over multiple runs is depicted in Fig. 19.

Based on the results displayed above, convergence has been achieved concerning the count of distinct repair actions. The total number of simulations has been specified at one million for all subsequent calculations, unless stated otherwise.

4.3. Quantification of different repair actions

Throughout the operational lifespan of a wind turbine blade, the model enables us to record the total count of distinct repair actions conducted. Concerning the defects monitored by inspection, Fig. 20(a) illustrates the average number of different repair actions. Type I and Type II repairs occur more frequently, while Type III and Type IV repairs are relatively less common. Since Type I and II generally incur lower repair costs, while Type III and IV have significantly higher repair costs, it is crucial for the monitoring system to promptly notify engineers of any detected failures. Engineers can then prioritize and carry out repairs to minimize the risk of defects degrading and incurring higher costs.

In Fig. 20(b), which represents the defects monitored by CM, no Type I repair actions are observed. This is because Type I repairs are exclusively conducted when more severe nearby defect is required to repair. Given that there is only one type of defect in the CM module, Type I actions cannot be initiated based on engineering knowledge provided in Table 1. The predominant repair actions are of Type II, while Type IV actions are less frequent and constitute the minority.

4.4. Assessing the monitoring system's reliability through probability distribution of state discovery

Monitoring outcomes are significantly influenced by the reliability or monitoring accuracy of the CM system. As discussed in Section 3.3, when the system detects defects, three potential scenarios can occur: underestimation, accurate reporting, and overestimation. Therefore, the identified state by the monitoring system may differ from the true state. The designed CM module is used for a comprehensive representation of misreporting.

Probability distributions of discovered states via the CM system for different true states are provided, as shown in Fig. 21. Please note that, in line with the aforementioned assumptions, false reporting can only result in a single state difference. This means that, for example, when state 2 is the true state, only states 1, 2, and 3 can be an output of the CM system. Referring to Fig. 21(a), it is evident that state 1 reporting exhibits an overall accuracy rate of approximately 87.96% with a probability of incorrect reporting of state 2 of 12.04%. As shown in Fig. 21(b), the monitoring accuracy progressively declines over time in accordance with the aging process following monitoring accuracy path 2, as depicted in Fig. 24. The overall monitoring accuracy of state 2, as shown in Fig. 21(c), is approximately 89.80%, with a probability of incorrect reporting to states 1 and 3 standing at 5.39% and 4.81%, respectively. This accuracy rate is consistent with that observed for state 1. Fig. 21(d) reveals that, initially, False state 1 constitutes a significant portion and exhibits a declining trend, followed by a gradual rise after reaching a minimum point. Error reporting for state 3 demonstrates a gradual upward trajectory. Similar patterns are also observed for state 3 and state 4.

Fig. 22 provides a comprehensive summary of the overall monitoring accuracy for different states, offering engineers a means of assessing the monitoring accuracy and state identification. Generally, the overall monitoring accuracy exhibits a decreasing trend from state 1 to state 5, with poorer states being identified with a lower monitoring accuracy.

4.5. Assessing the monitoring system's reliability through state discovery time

Time is a critical factor, as the inability to detect defects promptly may result in their further degradation, potentially incurring substantial costs. Furthermore, aside from monitoring accuracy, incorrect reporting introduces disparities in reported times compared to the actual degradation processes. Investigating this time gap holds significant value in expediting engineers' decision-making processes.

We have categorized the monitoring scenarios into three distinct groups. Group 1 signifies that the CM system detects degradation as it occurs, resulting in accurate and timely reporting. Group 2 indicates that the CM system detects degradation when no degradation has occurred. Group 3 implies that the CM system fails to detect degradation when it does indeed take place. For a more detailed illustration of this grouping, let us consider the example of state 2. In this instance:

- Group 1 represents the first monitoring interval after the wind turbine blade's defect has progressed from state 1 degradation to state 2, and the CM system successfully detects this change.
- Group 2 denotes a situation where the current state is state 2, but the CM system erroneously detects state 3 instead.
- Group 3 signifies that the current state is state 3, yet the CM system detects state 2.

To compute this time gap, we take the difference between the time when the actual state occurs and the time at which the monitoring system correctly or incorrectly reports. It is important to note that Group 2's monitoring reporting time will be set to 0 because there is no corresponding time for the true state, meaning that Group 2's monitoring reporting time is equivalent to the time step at which the CM system misreports a state. Consequently, Group 2's time gap is a positive value.

For Group 1, the time gap is either 0 or equals the negative monitoring interval. The reason for a time gap of 0 is that when the calculation commences, the first output time step of the program coincides with the first time step at which the monitoring transition fires in the PN module. Consequently, for the initial appearance of state 1, the time gap is 0, while for subsequent instances, it represents a negative value equivalent to the monitoring interval.

Group 3's time gap, on the other hand, is a negative integer multiple of the monitoring interval. The results are presented in figures in

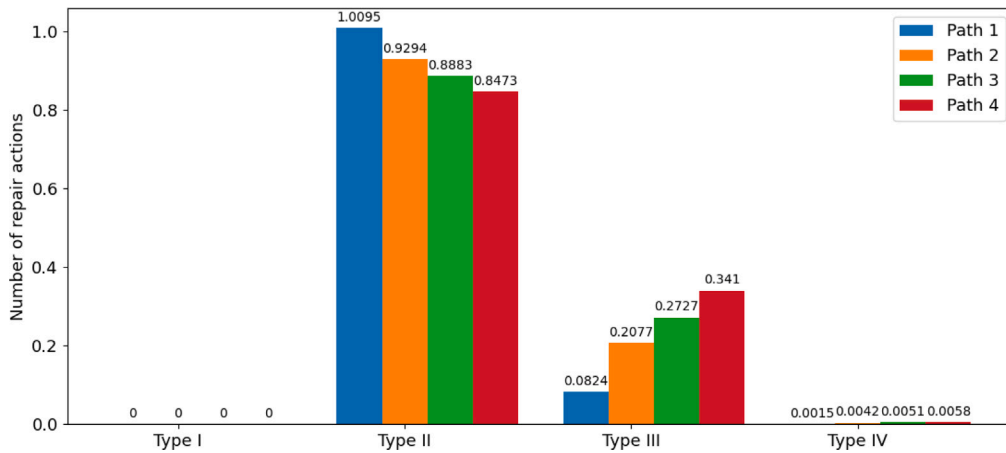


Fig. 25. Average number of different repair actions under different monitoring accuracy paths.

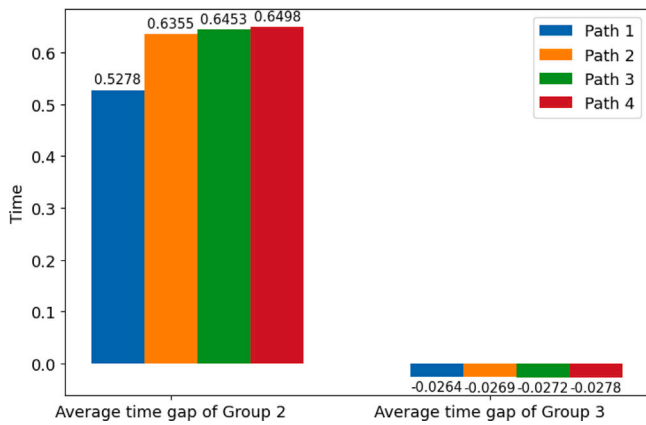


Fig. 26. Average time gap of Group 2 and Group 3 under different monitoring accuracy paths.

Fig. 23. The discovery time gap for state 1 is illustrated from Fig. 23(a) to (d). Analyzing Fig. 23(a), it is evident that Group 1 comprises the largest portion of the overall distribution, aligning with the simulation outcomes presented in the previous section. This indicates that the system operates normally with a high likelihood. Within Group 1, the probability of having a time gap of zero slightly exceeds -0.0125 . Group 2 exhibits a broader distribution, spanning from 0.0125 to 1. Among these values, the highest probability is observed within the range of 0.0125 to 0.1, followed by the interval between 0.6 and 0.7. This suggests that when the actual state is state 1, the erroneous reporting of state 2 primarily occurs during the early and middle stages of the simulation run. For Group 3, the distribution range is 0, signifying that there is no delay for state 1 reporting. Indeed, as for the designed PN, there is no possibility of delay for state 1 reporting.

The discovery time gap for state 2 is presented from Fig. 23(e) to (h). When comparing this to the discovery time gap for state 1, several distinctions become evident. In Group 1, only a time gap of -0.0125 is observed, indicating that state 2 is detected nearly immediately upon its occurrence. Group 2, on the other hand, displays a broader distribution, with the highest range being from 0.9 to 1.0, although the most concentrated part falls within the range of 0.3 to 0.9. This suggests that, in Group 2, reporting state 3 when the actual state is state 2 predominantly occurs within these time intervals. Within Group 3, the majority of time gaps are distributed at twice the monitoring interval. While other delays may occur, their probability diminishes as the length of the delay increases.

The discovery time gaps for state 3 and state 4 exhibit a similar pattern, with the primary distinction being the expansion of the time span in which Group 2 occurs most frequently. This observation aligns with the expectation that severe failure states typically manifest relatively later in the monitoring process.

In essence, the results presented here provide insights not only into the presence of errors in the monitoring system but also into the extent of its inaccuracy.

4.6. Examining the influence of the monitoring system's failure rate

Clearly, the failure of monitoring systems has a significant impact on the outcomes of asset management. Therefore, it is essential to understand how the failure rate of monitoring systems affects asset management results. We define the monitoring accuracy path to mirror the failure rate of the monitoring system. When the monitoring accuracy decreases at a faster rate, it indicates a higher failure rate for the monitoring system. Four monitoring accuracy paths are considered, as shown in Fig. 24. Path 1 maintains a constant monitoring accuracy over the entire lifetime. In contrast, the other three paths exhibit declining monitoring accuracy at varying rates. Path 4 signifies the least reliable monitoring system, experiencing the most significant decline in monitoring accuracy over time.

Fig. 25 illustrates the average number of different repair actions under various monitoring accuracy paths. It is evident that as aging accelerates, the number of Type II repair actions decreases, while the number of Type III and Type IV repair actions increases. When monitoring accuracy is high, the system can promptly detect degradation and notify engineers for timely maintenance, thus preventing further deterioration of the defect. It is crucial not to underestimate the increase in the number of Type III and Type IV repair actions. Their associated maintenance costs will escalate significantly in comparison to Type II repairs [40].

Fig. 26 presents the average time gap of Group 2 and Group 3 under various monitoring accuracy paths. It is observed that as the system ages more rapidly, the average time gap for both Group 2 and Group 3 increases. This indicates that the extent of misreporting becomes more pronounced as the system ages more rapidly.

5. Discussion

In this study, all input parameters have been standardized to a unit value in proportion to the lifespan of wind turbine blades due to the lack of data source. Therefore, the outputs of the PNs lack a direct physical interpretation in reality. For instance, the number of different repair actions in Fig. 20 represents the number of repairs over the normalized lifetime of wind turbine blades. However, the ratio of

the number of different repair actions is meaningful, as it provides a comparison between different strategies over the actual lifetime of wind turbine blades.

In real-life applications, identifying failure of the monitoring system can be challenging. Thus, the assessment of the monitoring system's reliability relies on assumed failure rates of the monitoring system in this study. The impact of the monitoring system's reliability on the asset management modelling output is reflected in the probability distribution of state discovery and state discovery time. The study also explores the influence of different failure rates on the number of different repair actions and the average time gap between the time when the actual state occurs and the misreporting time. These results provide valuable insights into the importance of considering the reliability of the monitoring system.

An enhancement to this methodology could involve using information theory to evaluate the expected information gain of the sensor network and employing PNs to model sensor network failures. This approach would provide a more accurate assessment of how the monitoring accuracy of the CM system changes over time [42], potentially enhancing the accuracy and practicality of the current study.

6. Conclusions

This paper introduces the development of an asset management PN model tailored for wind turbine blades, which integrates the SHM process and its reliability. The model is designed to incorporate industrial guidelines, enhancing its alignment with practical scenarios. The study conducted a comprehensive investigation into the influence of monitoring system reliability on asset management outcomes.

In summary, the paper presents a thorough analysis of true discovery states and incorrect reporting over time. This analysis shines a spotlight on the errors made by monitoring systems and their underlying causes. Additionally, the paper highlights the time gap associated with misreporting, illustrating the extent of these errors. Lastly, the study explores the impact of aging rates on reliability indicators. The findings emphasize the critical importance of reliability, providing valuable guidance for practical applications in the wind energy sector. In the future, the PN modules will undergo further enhancements by incorporating the failure rate of the monitoring accuracy evaluation scheme [42]. Additionally, maintenance cost considerations can be

taken into account. In the case of obtaining detailed CM system failure data, it is more realistic to use stochastic PNs to describe the CM system failure process, rather than using a constant transition rate to define the CM system failure process. Stochastic CM module will generate more accurate monitoring accuracy paths of the monitoring system. Finally, incorporating electricity production into the study would enable engineers to balance operational and management costs with the annual energy production of wind farms. Future research efforts will aim to integrate electricity production into the proposed asset management modelling.

CRedit authorship contribution statement

Wen Wu: Writing – original draft, Visualization, Validation, Software, Methodology, Investigation, Formal analysis, Conceptualization. **Darren Prescott:** Writing – review & editing, Validation, Supervision, Methodology, Investigation, Conceptualization. **Rasa Remenyte-Prescott:** Writing – review & editing, Validation, Supervision, Project administration, Funding acquisition, Conceptualization. **Ali Saleh:** Writing – review & editing, Validation, Software, Resources. **Manuel Chiachio Ruano:** Writing – review & editing, Validation, Supervision, Resources.

Declaration of competing interest

The authors declare that they have no known competing financial interests or personal relationships that could have appeared to influence the work reported in this paper.

Acknowledgements

This work has received funding from the European Union's Horizon 2020 research and innovation program under the Marie Skłodowska-Curie grant agreement No. 859957.

Appendix A. Summary of input parameters and places used in the PN models

See Tables A.2–A.5.

Table A.2
Summary of input parameters and places used in the CM PN module.

Transition name	Transition type	Transition parameters	Action
$T_{j,1}$	Weibull distribution	$\eta = 0.4935, \beta = 2.9000$ [33,41]	Failure state transition
$T_{j,2}$	Weibull distribution	$\eta = 0.1595, \beta = 2.1283$ [33,41]	Failure state transition
$T_{j,3}$	Weibull distribution	$\eta = 0.3838, \beta = 2.0020$ [33,41]	Failure state transition
$T_{j,4}$	Weibull distribution	$\eta = 0.4935, \beta = 2.9000$ [33,41]	Failure state transition
$T_{j,5}$	Probability transition	$B_{P_{j,6}} = 0.9, B_{P_{j,7}} = 0.1, F = 0.0125$	Perform monitoring
$T_{j,6}$	Probability transition	$B_{P_{j,6}} = 0.05, B_{P_{j,7}} = 0.9, B_{P_{j,8}} = 0.05, F = 0.0125$	Perform monitoring
$T_{j,7}$	Probability transition	$B_{P_{j,7}} = 0.05, B_{P_{j,8}} = 0.9, B_{P_{j,9}} = 0.05, F = 0.0125$	Perform monitoring
$T_{j,8}$	Probability transition	$B_{P_{j,8}} = 0.05, B_{P_{j,9}} = 0.9, B_{P_{j,10}} = 0.05, F = 0.0125$	Perform monitoring
$T_{j,9}$	Probability transition	$B_{P_{j,9}} = 0.1, B_{P_{j,10}} = 0.9, F = 0.0125$	Perform monitoring
$T_{j,10}$ – $T_{j,14}$	Immediate transition	$F = 0$	State discovery
$T_{j,15}$ – $T_{j,24}$	Immediate transition	$F = 0$	State updating
$T_{j,25}$ and $T_{j,28}$	Immediate transition	$F = 0$	Waiting for repair
$T_{j,26}$	Uniform distribution	$D_1 = 0.05, D_2 = 0.075$ [37]	Waiting for repair
$T_{j,27}$	Uniform distribution	$D_1 = 0.00625, D_2 = 0.0125$ [37]	Waiting for repair
$T_{j,29}$ and $T_{j,30}$	Immediate transition	$F = 0$	State updating
$T_{j,31}$ – $T_{j,34}$	Constant number	$F = 0.003125$	Perform repair
$T_{k,1}$	Constant number	$F = 0.3$	Failure state transition
$T_{k,2}$	Constant number	$F = 0.3$	Failure state transition
$T_{k,3}$	Constant number	$F = 0.3$	Failure state transition

Note: B denotes the probability of probability transitions, and the subscript of B denotes the specified place. F denotes the firing interval. D denotes the upper and lower bounds of uniform distributions.

Table A.3
Description of places used in the CM PN module.

Place name	Description
$P_{j,1}-P_{j,5}$	Actual defect severity of Rating 1, 2, 3, 4 and 5
$P_{j,6}-P_{j,10}$	Monitored defect severity by the CM system
$P_{j,11}-P_{j,15}$	Inhibit repeated reporting by the CM system
$P_{j,16}-P_{j,20}$	Identified defect ratings by the CM system
$P_{j,21}-P_{j,24}$	Start repair
$P_{j,25}-P_{j,28}$	Inhibit repeated repair actions
$P_{k,1}-P_{k,4}$	Degradation states of the CM system

Table A.4
Summary of input parameters and places used in the inspection PN module.

Transition name	Transition type	Transition parameters	Action
$T_{i,1}$	Weibull distribution	$\eta = 0.4935, \beta = 2.9000$ [33,41]	Failure state transition
$T_{i,2}$	Weibull distribution	$\eta = 0.1595, \beta = 2.1283$ [33,41]	Failure state transition
$T_{i,3}$	Weibull distribution	$\eta = 0.3838, \beta = 2.0020$ [33,41]	Failure state transition
$T_{i,4}$	Weibull distribution	$\eta = 0.4935, \beta = 2.9000$ [33,41]	Failure state transition
$T_{i,5}-T_{i,9}$	Immediate transition	$F = 0$	Perform inspection
$T_{i,10}-T_{i,14}$	Immediate transition	$F = 0$	State discovery
$T_{i,15}-T_{i,24}$	Immediate transition	$F = 0$	State updating
$T_{i,25}$ and $T_{i,28}$	Immediate transition	$F = 0$	Waiting for repair
$T_{i,26}$	Uniform distribution	$D_1 = 0.05, D_2 = 0.075$ [37]	Waiting for repair
$T_{i,27}$	Uniform distribution	$D_1 = 0.00625, D_2 = 0.0125$ [37]	Waiting for repair
$T_{i,29}-T_{i,30}$	Immediate transition	$F = 0$	State updating
$T_{i,31}-T_{i,34}$	Constant number	$F = 0.003125$	Perform repair
$T_{i,35}$	Probability transition	$B_{P_{i,29}} = 0.3, B_{P_{i,30}} = 0.2, B_{P_{i,31}} = 0.5, \eta = 4.05, \beta = 3.5$	Perform inspection
$T_{i,36}-T_{i,38}$	Immediate transition	$F = 0$	State discovery
$T_{x,\theta}$	Constant number	$F = 0.15$	Start inspection
$T_{x,i}$	Constant number	$F = 0.001$	Waiting for next inspection
$T_{i,n=1}$	Immediate transition	$F = 0$	State updating
$T_{i,n>1}$	Immediate transition	$F = 0$	State updating

Table A.5
Description of places used in the inspection PN module.

Place name	Description
$P_{i,1}-P_{i,5}$	Actual defect size range of Rating 1, 2, 3, 4 and 5
$P_{i,6}-P_{i,10}$	Identified defect ratings by the inspection
$P_{i,11}-P_{i,15}$	Inhibit repeated reporting by the inspection
$P_{i,16}-P_{i,20}$	Identified blade ratings by the inspection
$P_{i,21}-P_{i,24}$	Start repair
$P_{j,25}-P_{j,28}$	Inhibit repeated repair actions
$P_{i,29}$	Unclassified defect at root
$P_{i,30}$	Unclassified defect at mid span
$P_{i,31}$	Unclassified defect at tip
$P_{i,x}$	Defect i state change occurs
$P_{x,\sigma}$	At least one defect has changed state at least once
$P_{x,i}$	Between inspection
$P_{x,\theta}$	Inspection occurring

References

- [1] Wind industry reaches 1 terawatt wind energy capacity milestone. 2023, <https://www.gevwindpower.com/wind-industry-news/>.
- [2] Caous D, Bois C, Wahl J-C, Palin-Luc T, Valette J. Toward composite wind turbine blade fatigue life assessment using ply scale damage model. *Proc Eng* 2018;213:173–82.
- [3] Nielsen JJ, Sørensen JD. On risk-based operation and maintenance of offshore wind turbine components. *Reliab Eng Syst Saf* 2011;96:218–29.
- [4] Nielsen JSn, Sørensen JD. Computational framework for risk-based planning of inspections, maintenance and condition monitoring using discrete Bayesian networks. *Struct Infrastructure Eng* 2018;14:1082–94.
- [5] Marseguerra M, Zio E, Podofilini L. Condition-based maintenance optimization by means of genetic algorithms and Monte Carlo simulation. *Reliab Eng Syst Saf* 2002;77:151–65.
- [6] Márquez FPG, Tobias AM, Pérez JMP, Papaelias M. Condition monitoring of wind turbines: Techniques and methods. *Renew. Energy* 2012;46:169–78.
- [7] Hameed Z, Hong Y, Cho Y, Ahn S, Song C. Condition monitoring and fault detection of wind turbines and related algorithms: A review. *Renew Sustain Energy Rev* 2009;13:1–39.
- [8] Petri CA, Reisig W. Petri net. *Scholarpedia* 2008;3:6477.
- [9] Prescott D, Andrews J. A track ballast maintenance and inspection model for a rail network. *Proc Inst Mech Eng O: J Risk Reliab* 2013;227:251–66.
- [10] Yan R, Dunnett S. Improving the strategy of maintaining offshore wind turbines through Petri net modelling. *Appl Sci* 2021;11:574.
- [11] Müller F, Bertsche B. Availability analysis and maintainability optimization of an offshore wind farm using high-level Petri nets. *Forschung im Ingenieurwesen* 2021;85:639–48.
- [12] Santos F, Teixeira A, Guedes Soares C. Maintenance planning of an offshore wind turbine using stochastic Petri nets with predicates. *J Offshore Mech Arct Eng* 2018;140.
- [13] Le B, Andrews J. Modelling wind turbine degradation and maintenance. *Wind Energy* 2016;19:571–91.
- [14] Saleh A, Chiachío M, Salas JF, Kolios A. Self-adaptive optimized maintenance of offshore wind turbines by intelligent Petri nets. *Reliab Eng Syst Saf* 2023;231:109013.
- [15] Yan R, Dunnett S, Jackson L. Impact of condition monitoring on the maintenance and economic viability of offshore wind turbines. *Reliab Eng Syst Saf* 2023;109475.
- [16] Chiachío M, Chiachío J, Prescott D, Andrews J. Plausible Petri nets as self-adaptive expert systems: A tool for infrastructure asset monitoring. *Comput-Aided Civ Infrastruct Eng* 2019;34:281–98.
- [17] Naybour M, Remenye-Prescott R, Boyd MJ. Reliability and efficiency evaluation of a community pharmacy dispensing process using a coloured Petri-net approach. *Reliab Eng Syst Saf* 2019;182:258–68.
- [18] Liu S, Li W, Gao P, Sun Y. Modeling and performance analysis of gas leakage emergency disposal process in gas transmission station based on Stochastic Petri nets. *Reliab Eng Syst Saf* 2022;226:108708.
- [19] Saleh A, Remenye-Prescott R, Prescott D, Chiachío M. Intelligent and adaptive asset management model for railway sections using the iPN method. *Reliab Eng Syst Saf* 2024;241:109687.
- [20] Hadri O, Prescott D. Modular asset management framework based on Petri-net formalisations and risk-aware maintenance. *Reliab Eng Syst Saf* 2024;243:109828.
- [21] Yan R, Dunnett S, Andrews J. A Petri net model-based resilience analysis of nuclear power plants under the threat of natural hazards. *Reliab Eng Syst Saf* 2023;230:108979.
- [22] Reisig W. *Understanding petri nets*. Springer; 2016.
- [23] Nielsen JS, Tcherniak D, Ulriksen MD. A case study on risk-based maintenance of wind turbine blades with structural health monitoring. *Struct Infrastruct Eng* 2021;17:302–18.
- [24] Mukhopadhyay K, Liu B, Bedford T, Finkelstein M. Remaining lifetime of degrading systems continuously monitored by degrading sensors. *Reliab Eng Syst Saf* 2023;231:109022.
- [25] Nielsen L, Tølbø Il Glavind S, Qin J, Faber MH. Faith and fakes—dealing with critical information in decision analysis. *Civil Eng Environ Syst* 2019;36:32–54.
- [26] Ali K, Qin J, Faber MH. On information modeling in structural integrity management. *Struct Health Monit* 2022;21:59–71.
- [27] Qin J. Preposterior analysis considering uncertainties and dependencies of information relevant to structural performance. *ASCE-ASME J Risk Uncertain Eng Syst A* 2022;8:04021085.
- [28] Continuous non-contact blade damage detection system overview and results. 2021, <https://www.eologix-ping.com/en/>.
- [29] Joosse P, Blanch M, Dutton A, Kouroussis D, Philippidis T, Vionis P. Acoustic emission monitoring of small wind turbine blades. *J Sol Energy Eng* 2002;124:446–54.
- [30] Raišutis R, Jasiūnienė E, Žukauskas E. Ultrasonic NDT of wind turbine blades using guided waves. *Ultragarsas/Ultrasound* 2008;63:7–11.
- [31] Introducing the SkySpecs' ROVER. 2022, <https://skyspecs.com/wp-content/uploads/2022/05/Rover-by-Skyspecs.pdf>.
- [32] Wang L, Zhang Z. Automatic detection of wind turbine blade surface cracks based on UAV-taken images. *IEEE Trans Ind Electron* 2017;64:7293–303.
- [33] Wu W, Saleh A, Remenye-Prescott R, Prescott D, Chiachío M, Chronopoulos D. Asset management modelling approach integrating structural health monitoring data for composite components of wind turbine blades. In: *Proceedings of the 32nd European safety and reliability conference*. Research Publishing Services; 2022.
- [34] Murata T. Petri nets: Properties, analysis and applications. *Proc IEEE* 1989;77:541–80.
- [35] Chiachío M, Saleh A, Naybour S, Chiachío J, Andrews J. Reduction of Petri net maintenance modeling complexity via approximate Bayesian computation. *Reliab Eng Syst Saf* 2022;222:108365.
- [36] Lopez JC, Kolios A. Risk-based maintenance strategy selection for wind turbine composite blades. *Energy Rep* 2022;8:5541–61.
- [37] *Wind turbine blades handbook*. 2021, <https://www.bladena.com>.
- [38] Brouwer SR, Al-Jibouri SH, Cárdenas IC, Halman JI. Towards analysing risks to public safety from wind turbines. *Reliab Eng Syst Saf* 2018;180:77–87.
- [39] Datsiou KC, Overend M. Weibull parameter estimation and goodness-of-fit for glass strength data. *Struct Saf* 2018;73:29–41.
- [40] Mishnaevsky Jr. L, Thomsen K. Costs of repair of wind turbine blades: Influence of technology aspects. *Wind Energy* 2020;23:2247–55.
- [41] Li X, Kupski J, De Freitas ST, Benedictus R, Zarouchas D. Unfolding the early fatigue damage process for CFRP cross-ply laminates. *Int J Fatigue* 2020;140:105820.
- [42] Wu W, Cantero-Chinchilla S, Prescott D, Remenye-Prescott R, Chiachío M. A general approach to assessing SHM reliability considering sensor failures based on information theory. *Reliab Eng Syst Saf* 2024;250:110267.